Vacancy-induced structures in the angle-resolved photoemission spectra of substoichiometric $TiN_x(100)$

J. Redinger* and P. Weinberger
Institut für Technische Elektrochemie, Technische Universität Wien, A-1060 Wien, Austria

A. Neckel
Institut für Physikalische Chemie, Universität Wien, A-1090 Wien, Austria
(Received 30 January 1986; revised manuscript received 24 November 1986)

Angle-resolved uv photoemission spectra (ARUPS) are calculated for substoichiometric $TiN_x(100)$, $x=0.83$ and 0.92, for different geometries of the incident photons and for a variety of incident photon energies. Vacancy-induced structures show up distinctly in normal emission for photon energies above 36 eV. For off-normal ARUPS such structures are found even in the typical UPS regime (Ne I, He I). In contrast to our theoretical predictions and in contrast to measured angle-integrated UPS and x-ray photoemission spectra, recent experimental ARUPS for $TiN_{0.83}(100)$ give no evidence of vacancy-induced structures, neither in normal nor in off-normal emission. A surface-induced feature was detected instead.

I. INTRODUCTION

Angle-resolved photoemission has proved to be one of the most powerful techniques for probing the electronic structure of solid matter. In particular, the use of synchrotron radiation has tremendously enlarged the applicability of photoemission experiments. In the present paper a method (Redinger *et al.*[1]) is applied that allows the calculation of the photocurrent for disordered complex lattices. This method is an extension of the theory of photoemission for disordered binary alloys as discussed by Durham,[2] which, in turn, is based on the theoretical concepts given by Pendry.[3,4] For ordered multisublattice systems, theoretical photocurrent calculations were performed for the first time for CuZn(110) (Durham *et al.*,[5] Larsson[6]) and using *ab initio*—like surface potentials for TiC(100) (Redinger *et al.*[7]).

For refractory phases, i.e., carbides and nitrides of Ti, V, Nb, Zr, etc., there seems to be a severe discrepancy between the experimental measurements in the x-ray-photoemission spectroscopy (XPS) and the Ultraviolet-photoemission spectroscopy (UPS) regimes. In the XPS regime a pronounced vacancy-induced peak appears both in experimental (Höchst *et al.*,[8] Porte *et al.*[9]) and theoretical (Redinger *et al.*[10]) spectra. It is worthwhile to note that the XPS experiments have been performed using different kinds of samples. The spectra by Höchst *et al.*[8] were obtained from a bulky polycrystal, whereas Porte *et al.*[9] employed thin polycrystalline films. In the UPS regime, however, the situation is somewhat controversial. Vacancy-induced features have been seen in angle-integrated UPS spectra from polycrystalline $TiN_{0.80}$ (Bringans and Höchst[11]), while both angle-integrated and angle-resolved spectra recorded on $TiN_{0.83}(100)$ single crystals failed to reproduce any vacancy-related structure (Johansson *et al.*[12,13]). In the case of the angle-resolved spectra, a Tamm surface state has been identified (Johansson and Callenas,[14] Inglesfield *et al.*[15]). Up to now, the angle-resolved spectra for $TiN_{0.83}(100)$—both bulk and surface-related peaks—have been, surprisingly enough, successfully interpreted using a stoichiometric model of photoemission (Larsson *et al.*,[16] Johansson *et al.*[17]). It seems, however, that not only a proper description of the composition of the nonstoichiometric samples is needed for an interpretation of photoemission data, but also an adequate model for concentration-dependent reconstructions in the first few layers of the crystal. Strong indications for such concentration-dependent reconstructions were found experimentally from He scattering on TiC_x surfaces (Aono *et al.*[18]).

The present paper has to be understood as a kind of "piloting study," since most of the refractory phases are notoriously nonstoichiometric and, also, since similar problems such as antistructural atoms in pseudobinary or ternary alloys can arise in quite a different context.

II. COMPUTATIONAL DETAILS

Within the framework of the coherent-potential approximation (CPA), the photocurrent emerging from a substitutionally disordered alloy can be split into a coherent and an incoherent contribution (Durham[2]). The coherent part contains the k-dependent information, whereas the incoherent part arises from fluctuations of the random system about the effective coherent lattice and involves only site-diagonal information on the initial states. The calculation of the coherent contribution is completely analogous to a calculation of the photocurrent for an ordered alloy,[6,19] except that effective CPA matrix elements and effective CPA scattering amplitudes are used instead of only local-potential-dependent matrix elements and phase shifts. In the present case of a pseudobinary alloy, the incoherent contribution to the photocurrent is obtained using the configuration-averaging procedure as given by Schadler *et al.*[20]

All spectra shown in this paper are based on Korringa-

Kohn-Rostoker (KKR) - CPA scattering amplitudes for the ground-state (Marksteiner *et al.*[21]) and ATA (averaged—t-matrix approximation) -like scattering amplitudes for the excited state. This kind of setup for the excited states was already successfully used by Durham[2] for simple lattice substitutional alloys.

Just as in the case of stoichiometric TiN,[16,17] bulk lattice parameters are assumed even for the surface layer, and the surface potential barrier is located such that it touches the muffin-tin spheres in the surface layer. The height of the surface barrier is chosen to be 14.9 eV with respect to the muffin-tin zero and is the same for all vacancy concentrations. To ensure convergence, 21 reciprocal-lattice vectors are included in the calculation. The electron and hole lifetime-broadening parameters are chosen to be -2.0 and -0.14 eV for the high- and low-energy states, respectively. These broadening parameters are, in particular, used to match the present calculation with the previous calculation for stoichiometric TiN(100).[16,17] The applied parameters are not optimized values, but seem to be reasonable estimates as judged by the experience gained in other calculations (Larsson,[22] Pendry and Hopkinson,[23] Redinger *et al.*[7]). Finally, the calculated spectra have been convoluted with a Gaussian spectrometer function (a full width at half maximum of 0.2 eV) and are normalized to the largest peak.

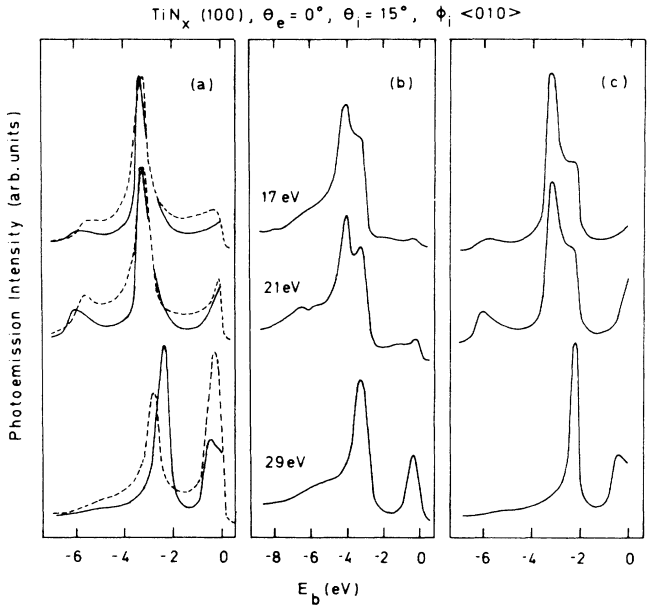

FIG. 1. Normal-emission spectra for $TiN_x(100)$ using p-polarized light incident at 15° relative to the surface normal along the ⟨010⟩ azimuth: (a) calculated spectra $x=0.83$ (dashed line), $x=1.0$ from Ref. 16 (solid line), (b) Experimental spectra from Ref. 13, and (c) calculated spectra (Ref. 16) for $x=1.0$ using a modified surface potential.

III. RESULTS

A. Normal emission

In Fig. 1 the present calculation for $TiN_{0.83}(100)$ [Fig. 1(a), dashed line] is compared with experimental data for $TiN_{0.83}(100)$ [Fig. 1(b)] and theoretical calculations for stoichiometric TiN(100) using different surface potentials [Fig. 1(a), solid line, and Fig. 1(c), respectively]. The calculations correspond to p-polarized light incident along the ⟨010⟩ azimuth at an angle $\theta_i=15$ with respect to the surface normal. Since in normal emission the final state has to be total symmetric (Δ_1), the component of the electromagnetic field parallel to the surface excites only Δ_1-like initial states and the component normal to the surface only Δ_5-like initial states. Thus, by increasing the angle of incidence, the emission from Δ_1-like states is enhanced relative to the emission from Δ_5-like states.

Roughly speaking, we obtain three peaks, one at an energy approximately between -6 and -5 eV, another one at about -3 eV, and a third just below the Fermi level (zero of energy). From the θ_i dependence it follows that the lowest peak arises from Δ_1-like N p initial states, whereas the other two features originate from Δ_5-like N p and Ti d initial states, respectively. Since the dispersion of the peaks follows quite nicely the bulklike initial bands along the $\Gamma-\Delta-X$ direction, direct transitions seem to be dominant for stoichiometric as well as for nonstoichiometric systems.

As compared to the experimental data [Fig. 1(b)] and the "stoichiometric" calculation for TiN(100) [Fig. 1(c)], there is no surface-induced peak at about 0.7 eV above the Δ_5-like N p band in the nonstoichiometric case. This Tamm surface state (Inglesfield *et al.*,[15] Larsson *et al.*[16]) originates from a different charge transfer at the surface due to the breaking of bonds. For ordered systems, Tamm states can be described theoretically by using *ab initio*—like surface potentials[7] or simply by shifting the top-layer potential by some constant [Fig. 1(c)]. For nonstoichiometric systems the situation is more complex: Firstly, *ab initio* calculations including surface vacancies are not available. Secondly, a shift of the top-layer potential is only possible for a stoichiometric top layer, since (at present) the potential employed in the calculation of the spectra has to be the same as that used for the calculation of the bulk CPA scattering amplitudes. Thirdly, because of additional broken bonds due to vacancies, surface vacancies will certainly strongly influence a Tamm surface state. In view of these reasons we did not attempt to incorporate top-layer potential-dependent effects for substoichiometric $TiN_{0.83}(100)$.

Nonstoichiometry introduces certain features which cannot be "observed" in the corresponding stoichiometric system. The intensity of the Δ_5-like N p peak is reduced with respect to the Ti d—like peak close to E_F. This reduction is most pronounced at a photon energy of 29 eV, where states corresponding to $\mathbf{k}$ points near the Brillouin-zone center are mapped. For $\mathbf{k}$ vectors in this particular region of the Brillouin zone, the N p band is at lower energies and the dispersion of the band is reduced. The upward shift of the Δ_1-like emission is largely due to a lowering of E_F by about 0.3 eV when going from $TiN_{1.0}$ to $TiN_{0.83}$. For photon energies below 36 eV the intensity

is only slightly enhanced in the energy region of the vacancy-induced features (around -2 eV).

As compared to the experimental data, the theoretical peak positions are found to be too high in energy. This kind of discrepancy, however, reflects nothing but the well-known problem of identifying local-density eigenvalues with quasiparticle excitations (see, e.g., Perdew[24]). Such discrepancies also occur in the calculated spectra for $TiN_{1.0}(100)$.[16,17] Nevertheless, we have to state that experimental spectra taken from a nominal $TiN_{0.83}(100)$ crystal seem to be in a better overall agreement with calculated angle-resolved ultraviolet photoemission spectroscopy (ARUPS) for stoichiometric TiN(100) rather than with those for substoichiometric $TiN_{0.83}(100)$.

Turning now to the spectra in Fig. 2, one can see that an additional vacancy-induced structure at about -2 eV comes into play for photon energies above 36 eV. Unfortunately, only angle-integrated data from a $TiN_{0.80}$ polycrystal are available in this photon-energy range. These spectra clearly show a -2 eV structure which is not present in the stoichiometric counterparts. This additional structure has been attributed to vacancy-induced states.[11] It should be mentioned that a vacancy-induced -2 eV peak was also found for substoichiometric TiN_x in the x-ray-photoemission spectroscopy (XPS) regime.[8–10]

Very recently, this peak was also found experimentally as well as theoretically for substoichiometric $ZrN_x(100)$.[25,26] By comparing Fig. 2(b) with Fig. 2(c) one can see that the intensity of the vacancy-induced peak decreases with decreasing vacancy concentration. No dispersion is detectable for the vacancy-induced structure at -2 eV. The intensity of the peak depends strongly on θ_i and is enhanced for larger values of θ_i, which, in turn, implies Δ_1-like symmetry. This is in accordance with an augmented-plane-wave (APW) supercell calculation for $TiN_{0.75}$ (Herzig *et al.*[27]), assuming an ordered defect structure.

The question now arises as to why this -2-eV vacancy peak is seen only for photon energies above 36 eV. To answer this question, one must consider both the initial and final states. From Bloch spectral functions for $TiN_{0.75}$, one can see that the vacancy states along the $\Gamma-\Delta-X$ line are particularly pronounced at k values greater than 0.5 (the X point is at 1.0). This part of the Brillouin zone is certainly probed with 17-eV photons (see the band structure of TiN shown in Fig. 1 of Johansson *et al.*[13]). Contrary to the shape of the Bloch spectral functions, however, around -2 eV, as compared with the spectra from stoichiometric TiN(100), only an increase in the "background" is observed. By increasing the photon energy one moves along an almost free-electron-like final state and approaches the Γ point around a photon energy of 30 eV. The inverse low-energy electron-diffraction (LEED) final state used in our calculations shows the same dispersion as the bulklike final state. It is rather sharp, and thus guarantees a good **k**-space resolution. This is reflected in Fig 2, where the emissions from the Δ_1-like and Δ_5-like N p initial states coincide for a photon energy of 33 eV. Increasing the photon energy further, one can see from the bulk band structure that after a short steep rise the Δ_1 final-state band becomes very flat. Because of this flattening seen in the three-dimensional

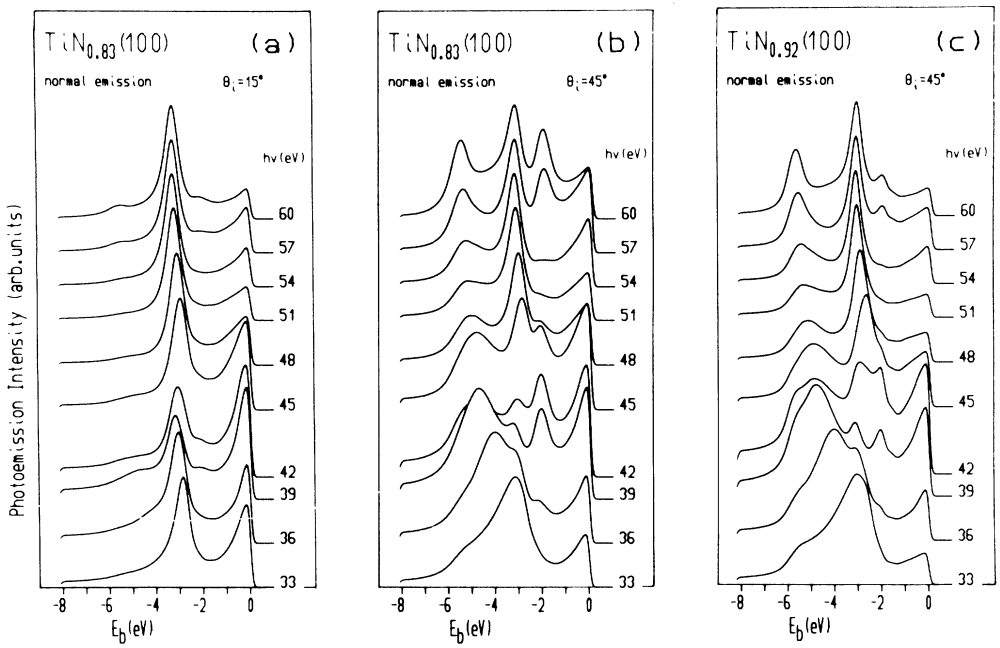

FIG. 2. Calculated normal-emission spectra for the experimental composition of $TiN_{0.83}(100)$ and $TiN_{0.92}(100)$. p-polarized light, with energies ranging from 33 up to 60 eV, is incident along the $\langle 010 \rangle$ azimuth at an angle relative to the surface-normal: (a) $x=0.83$, $\theta_i=15°$ (predominantly Δ_5 states); (b) $x=0.83$, $\theta_i=45°$ (both Δ_1 and Δ_5 states); (c) $x=0.92$, $\theta_i=45°$ (both Δ_1 and Δ_5 states). For photon energies above 36 eV the vacancy-induced structure at -2 eV is clearly visible for $\theta_i=45°$.

final-state band structure, the disorder broadening and the finite lifetime due to inelastic-scattering events become important for the LEED final state. This has two major consequences: (1) the **k**-space resolution is poor, which implies that also the second half of the $\Gamma-\Delta-X$ line is "seen," and (2) the coherence length becomes small, which, in turn, implies that mostly single-site (i.e., atomic-like) contributions are important for the photocurrent. Since the vacancy initial states are rather localized, this particular final-state situation causes their intensity to remain unchanged, whereas the intensity from the itinerant N p initial bands is radically quenched.

This is in contrast to the situation at lower photon energies, where the LEED final state is seen to be rather sharp. Although the relevant **k** region is probed, for lower photon energies the huge multiple-scattering contribution from the N p initial bands buries the vacancy peak in the "background." Pushing the photon energy beyond 48 eV, the vacancy peak disappears, but reappears again at 57 eV. The nature of the final state is again responsible for this intensity modulation. At about 48 eV the strongly broadened final state sharpens and again shows free-electron-like dispersion until the X point is reached at about 60 eV. The final state is particularly sharp for Δ points between 0.35 and 0.7 and shows a considerable broadening near the X point. Consequently the **k** resolution is rather good for photon energies around 50 eV, where initial vacancy states corresponding to Δ points around 0.5 could cause the emission at -2 eV. However, precisely in this **k**-point region the vacancy-induced initial states are not very well defined. For photon energies above 55 eV the final states again pick up the relevant portion of the Δ line. Now, again the final states are broadened sufficiently enough in order to quench the multiple-scattering contributions with respect to the N p–like initial states.

B. Polar-angle dependence

In order to study the photoemission for sub-stoichiometric $TiN_{0.83}(100)$ as a function of the electron-emission angle θ_e (polar angle) along the $\langle 011 \rangle$ azimuth, we carried out calculations for unpolarized Ne I (16.85 eV) and He I (21.2 eV) radiation. With this particular setup, initial states in the $\Gamma-X-U-L-K$ plane of the Brillouin zone are probed.

In Fig. 3 the dispersion of the calculated peaks (lines) for $TiN_{0.83}(100)$ is compared to the experimental peak positions[13] (circles). Since the results for Ne I and He I radiation are very similar, only the He I "bands" are displayed. Let us focus first on the energy region between E_F and -3 eV. For $\theta_e > 10°$ the vacancy-induced states (solid line) show up as a separate peak. This peak is most pronounced for $\theta_e > 20°$. For $\theta_e < 10°$ the peak turns into a very weak shoulder and vanishes completely for $\theta_e < 4°$. The dispersion of the vacancy peak is about 0.85 eV and shows a minimum binding energy of -1.65 eV around $\theta_e = 35°$ and a maximum of -2.4 eV at $\theta_e = 74°$.

This, at first sight, striking difference between normal and off-normal emission can be interpretated partially in terms of the band structure of stoichiometric TiN (cf. Fig. 1 of Ref. 13). Along [100], the N p and Ti d initial-state bands overlap, whereas for off-normal directions in the $\Gamma-X-U-L-K$ plane, away from $\Gamma-\Delta-X$, a gap opens. The APW supercell calculation for ordered $TiN_{0.75}$ shows that the vacancy states are predominantly found within this gap. In the disordered case the vacancylike states remain rather sharp, as can be seen by comparing the Bloch spectral functions for disordered $TiN_{0.75}$ along the $\Gamma-\Sigma-K$ direction (gap) with those along the $\Gamma-\Delta-X$ direction (no gap). Since this gap is also rather broad, there are no other initial states near by which as in the case of normal emission can overshadow the vacancy-state emission. It is therefore not surprising that the vacancy states are well resolved in off-normal emission, even for low photon energies.

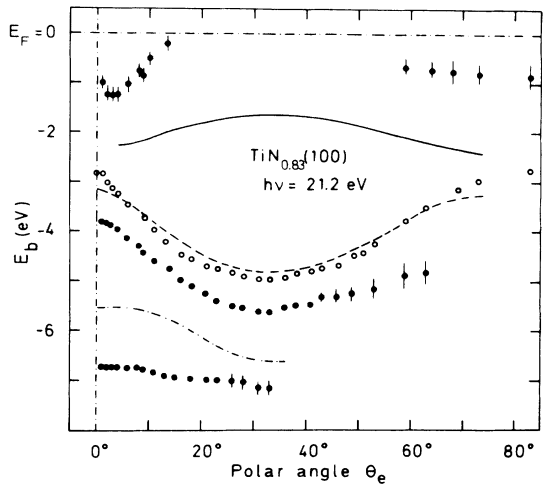

FIG. 3. Polar-angle (θ_e) dependence of the peak positions in the $\Gamma XULK$ plane for $TiN_{0.83}(100)$ using unpolarized He I (21.2 eV) radiation. Circles: experimental data from Ref. 13. Lines: present calculation.

The experimental "band" around -1 eV, as seen for polar angles $\theta_e < 15°$ and $\theta_e > 60°$, is not present in the calculated off-normal spectra for $TiN_{0.83}(100)$. This "band" was assigned to states derived from Δ_2'-like initial states for stoichiometric TiN. Its intensity is "weak" in the experimental spectra for $TiN_{0.83}(100)$ and in the calculated spectra for stoichiometric TiN(100).[17] These Δ_2'-like states are seen to be heavily affected by disorder. They remain sharp only in the vicinity of the Brillouin-zone center and near the X point, as discussed in Ref. 20. The disorder broadening seems to be large enough to rub out this spectral feature, even for $TiN_{0.83}(100)$.

As in the case of normal emission, the experimentally found surface state (open circles) is not present in the calculated spectra (cf. the discussion given for Fig. 1). The experimental "band" derived from Δ_5-like N p bulk states is found between -3.8 and -5.6 eV (solid circles), whereas the calculated counterpart (dashed line) is found between -3.15 and -4.85 eV. This almost constant offset of about 0.7 eV reflects the well-known problem of identifying local-density eigenvalues with quasiparticle excitations.[24] At around -6 eV the calculated band (dashed-dotted line) derived from Δ_1-like N p bulk states

appears. The corresponding experimental "band" (solid circles) is located at about -7 eV. As regards the dispersion of this band, the agreement with experiment is worse than for the Δ_5-like states.

IV. CONCLUSION

The present paper very clearly shows that vacancy-induced structures in the angle-resolved photoemission spectra for $TiN_{0.83}(100)$ should indeed be observable. Such structures were observed in a recent paper by Bringans and Höchst[11] in 40-eV angle-integrated spectra for polycrystalline $TiN_{0.80}$. Johansson *et al.*,[12] however, did not trace any such structure in their angle-integrated He II spectrum for a $TiN_{0.83}(100)$ single crystal. Since exactly the same crystal was used for their angle resolved study,[13] it is not at all surprising that their angle-resolved spectra do not show any vacancy-induced peaks. It is quite possible the vacancy-induced structures are missing because they essentially measured a nonstoichiometric sample with stoichiometric top layers. In the case of $TiC_x(100)$, Aono *et al.*[18] showed that the presence of vacancies in the surface region depends crucially on the temperature of the heat flashes used to clean the surface.

Recent measurements for $ZrN_x(100)$ by Johansson and co-workers[25] indeed show quite clearly the existence of vacancy-induced structures, confirming the correctness of our theoretical approach.[1,26]

In order to study the effects of a concentration gradient for the top layers, we have extended our scheme to handle different concentrations in different layers (Redinger and Weinberger[28]). We believe that a single stoichiometric top layer is sufficient to fake a "stoichiometric sample."

Note added in proof. A new synchrotron-based investigation of the substoichiometric TiN(100) surface by the Johansson group [P.A.P. Lindberg, L. I. Johansson, J. B. Lindström, and D. S. L. Law (unpublished)] revealed a vacancy-induced structure at -2.1 eV. This structure is visible in normal emission for photon energies above 30 eV.

ACKNOWLEDGMENT

This paper was partially supported by the Austrian Fonds zur Förderung der wissenschaftlichen Forschung (Projekt No. P5543). We are most grateful to Dr. P. J. Durham, Science and Engineering Research Council (SERC) Laboratory, Daresbury, United Kingdom, for very helpful discussions and for his continuous interest in our work.

*Present address: Department of Physics, Northwestern University, Evanston, IL 60201.

[1] J. Redinger, P. Weinberger, and A. Neckel (unpublished).
[2] P. J. Durham, J. Phys. F **11**, 2475 (1981).
[3] J. B. Pendry, *Low Energy Electron Diffraction* (Academic, New York, 1974).
[4] J. B. Pendry, Surf. Sci. **57**, 679 (1976).
[5] P. J. Durham, W. M. Temmerman, C. G. Larsson, and P. O. Nilsson, Vacuum **33**, 771 (1983).
[6] C. G. Larsson, Surf. Sci. **152/153**, 213 (1985).
[7] J. Redinger, P. Weinberger, E. Wimmer, A. Neckel, and A. J. Freeman, Phys. Rev. B **32**, 6993 (1985).
[8] H. Höchst, R. D. Bringans, P. Steiner, and Th. Wolf, Phys. Rev. B **25**, 7183 (1982).
[9] L. Porte, L. Roux, and J. Hanus, Phys. Rev. B **28**, 3214 (1983).
[10] J. Redinger, P. Marksteiner, and P. Weinberger, Z. Phys. B **63**, 221 (1986).
[11] R. D. Bringans and H. Höchst, Phys. Rev. B **30**, 5416 (1984).
[12] L. I. Johansson, P. M. Stefan, M. L. Shek, and A. N. Christensen, Phys. Rev. B **22**, 1032 (1980).
[13] L. I. Johansson, A. Callenås, P. M. Stefan, A. N. Christensen, and K. Schwarz, Phys. Rev. B **24**, 1883 (1981).
[14] L. I. Johansson and A. Callenås, Solid State Commun. **42**, 299 (1981).
[15] J. E. Inglesfield, A. Callenås, and L. I. Johansson, Solid State Commun. **44**, 1321 (1982).
[16] C. G. Larsson, L. I. Johansson, and A. Callenås, Solid State Commun. **49**, 727 (1984).
[17] L. I. Johansson, C. G. Larsson, and A. Callenås, J. Phys. F **14**, 1761 (1984).
[18] M. Aono, Y. Hou, R. Souda, C. Oshima, S. Otani, and Y. Ishizawa, Phys. Rev. Lett. **50**, 1293 (1983).
[19] J. F. L. Hopkinson, J. B. Pendry, and D. J. Titterington, Comput. Phys. Commun. **19**, 69 (1980).
[20] G. Schadler, P. Weinberger, A. Gonis, and J. Klima, J. Phys. F **15**, 1675 (1985).
[21] P. Marksteiner, P. Weinberger, A. Neckel, R. Zeller, and P. H. Dederichs, Phys. Rev. B **33**, 812 (1986).
[22] C. G. Larsson, Ph.D. thesis, Chalmers University of Technology, Gothenburg, 1982 (ISBN 91-7032-078-0).
[23] J. B. Pendry and J. F. L. Hopkinson, J. Phys. (Paris) Colloq. **39**, C4-142 (1978).
[24] J. P. Perdew, in *Density Functional Methods in Physics*, NATO Advanced Study Institute Series B 123, edited by R. M. Dreizler and J. da Providencia (Plenum, New York 1985), pp. 265—308.
[25] J. Lindström, L. I. Johansson A. Callenås, D. S. L. Law, and A. N. Christensen (unpublished).
[26] J. Redinger, Solid State Commun. **61**, 133 (1987).
[27] P. Herzig, J. Redinger, R. Eibler, and A. Neckel, in Proceedings of the Eighth International Conference on Solid Compounds of Transition Elements, April 9—13, 1985, Vienna, Austria (Extended Abstracts P2B2) (unpublished).
[28] J. Redinger and P. Weinberger, following paper, Phys. Rev. B **35**, 5652 (1987).